

# Cross-Coupling of Cobalt-Complexed Propargyl Radicals: Metal Core- and $\alpha$ - and $\gamma$ -Aryl-Induced Chemo- and Diastereoselectivity<sup>†</sup>

Gagik G. Melikyan,\* Arthur Floruti, Lucin Devletyan, Pogban Toure, Norman Dean, and Louis Carlson

Department of Chemistry and Biochemistry, California State University Northridge,  
Northridge, California 91330-8262

Received February 26, 2007

Chemo- and diastereoselectivities of homo- and cross-coupling reactions of  $\text{Co}_2(\text{CO})_6$ -complexed propargyl radicals were studied. The alternative radical generation methods—reduction of respective cations with Zn or  $\text{Cp}_2\text{Co}$  and one-step mediation with THF or  $\text{Tf}_2\text{O}$ —were employed. In the case of cobalt complexes with terminal triple bonds, the product distribution is nearly statistical and dependent upon the reducing agent with the concentration of the cross-coupling product **8** falling in the range 38–49%. The diastereoselectivity varied widely (de 40–92%) with the preponderant formation of *d,l*-diastereoisomers **7–9** in both homo- and cross-coupling reactions. The highest level of stereocontrol was achieved in THF- and  $\text{Tf}_2\text{O}$ -mediated reactions (de up to 92%), while the reductions with  $\text{Cp}_2\text{Co}$  were inferior in both homo- and cross-coupling processes (de 40–56%). An introduction of a  $\gamma$ -aromatic ring revealed a *kinetic differentiation at the radical generation step* that, in turn, resulted in a nonstatistical distribution of homo- and cross-dimers. The *d,l*-diastereoselectivity is found to be systematically lower for homo-dimer **16**, containing a  $\gamma$ -phenyl substituent at the triple bond (de: **16** 14–64%; **7** 52–84%). The observed chemoselectivities are accounted for on the basis of the computed values of charge distribution in the requisite cations.

## Introduction

The ability to control the chemo-, regio-, and stereoselectivity of radical reactions remains one of the main challenges of modern synthetic chemistry.<sup>1</sup> Among innovative approaches is the coordination of organic moieties with transition metals, which facilitates the generation of radical species and provides for their moderation.<sup>2</sup> The very topology of metal complexes allows for altering of the electronic, steric, and conformational parameters of  $\pi$ - and  $\sigma$ -bonded ligands by varying the nature of the transition metal, its oxidation state, and attendant with it, the mode of interaction with an organic moiety.<sup>2</sup> The

chemistry of organometallic radicals, in particular those with an unpaired electron localized on the  $\alpha$ -carbon atom in a  $\pi$ -bonded ligand, has become an emerging interdisciplinary field.<sup>2f</sup> The synthetic potential uncovered so far is truly remarkable: it provides novel methods for inter- and intramolecular radical C–C bond formation that readily occurs, in a selective manner, in a diverse polyfunctional environment.<sup>2d–f,3</sup> *Intermolecular homo-coupling radical reactions* constitute the bulk of the experimental material reported so far with a diastereomeric excess varying in the range 0–94%.<sup>3,4</sup> The

\* Corresponding author. E-mail: gagik.melikyan@csun.edu.

<sup>†</sup> This paper is dedicated to the memory of Dr. Alexander Tatoyan (1952–2004), a talented scientist, a colleague, and a friend.

(1) (a) Curran, D. P. In *Comprehensive Organic Synthesis*; Trost, B. M., Ed.; Pergamon Press: London, 1992, Vol. 5, pp 716, 780. (b) Malacria, M. *Chem. Rev.* **1996**, *96*, 289. (c) Giese, B.; Kopping, B.; Gobel, T.; Dickhaut, J.; Thoma, G.; Kulicke, K. J.; Trach, F. In *Organic Reactions*; Paquette L., Ed.; John Wiley: New York 1996; Vol. 48, p 301. (d) Curran, D. P.; Porter, N. A.; Giese, B. *Stereochemistry of Radical Reactions*; VCH: Weinheim, 1997. (e) Sibi, M. P.; Porter, N. A. *Acc. Chem. Res.* **1999**, *32*, 163. (f) Stereoselective Radical Reactions. Sibi, M. P.; Ternes, T. R. In *Modern Carbonyl Chemistry*; Otera, J., Ed.; Wiley-VCH: New York, 2000. (g) *Radicals in Organic Synthesis*; Sibi, M., Ed.; Wiley: New York, 2001; Vol. 1. (h) Zard, S. Z. *Radical Reactions in Organic Synthesis*; Oxford University Press, Inc.: New York, 2003; 256 pp. (i) Togo, H. *Advanced Free Radical Reactions for Organic Synthesis*; Elsevier: Amsterdam, 2004; 258 pp.

(2) (a) *Organometallic Radical Processes*; Trogler, W. C., Ed.; Elsevier: Amsterdam, 1990; Chapters 3, 4, 9, 10. (b) Collman, J. R.; Hegedus, L. S.; Norton, J. R.; Finke, R. G. *Principles and Applications of Organotransition Metal Chemistry*; University Science Books: Mill Valley, CA, 1987. (c) Astruc, D. *Acc. Chem. Res.* **1991**, *24*, 36. (d) Astruc, D. *Electron Transfer and Radical Processes in Transition-Metal Chemistry*; VCH: New York, 1995; Chapters 3, 5, 6. (e) Torraca, K. E.; McElwee-White, L. *Coord. Chem. Rev.* **2000**, *206–207*, 469. (f) Melikyan, G. G. In *Frontiers in Organometallic Chemistry*; Nova Science Publishers: New York, 2006; p 155, and references therein.

(3) (Pentadienyl radical)Fe(CO)<sub>5</sub>: (a) Mahler, J. E.; Gibson, D. H.; Pettit, R. *J. Am. Chem. Soc.* **1963**, *85*, 3959. (b) Sapienza, R. S.; Riley, P. E.; Davis, R. E.; Pettit, R. *J. Organomet. Chem.* **1976**, *121*, C35. (c) Pearson, A. J.; Chen, Y.-S.; Daroux, M. L.; Tanaka, A. A.; Zettler, M. J. *Chem. Soc., Chem. Commun.* **1987**, 155. (d) Hwang, W. S.; Liao, R. L.; Horng, Y. L.; Ong, C. W. *Polyhedron* **1989**, *8*, 479. (propargyl radical)Cp<sub>2</sub>Mo<sub>2</sub>(CO)<sub>4</sub>: (e) Le Berre-Cosquer, N.; Kergoat, R.; L'Haridon, P. *Organometallics* **1992**, *11*, 721. (benzyl radical)Cr(CO)<sub>3</sub>: (f) Top, S.; Jaouen, G. *J. Organomet. Chem.* **1987**, *336*, 143. Ferrocenyl radical: (g) Cais, M.; Eisenstadt, A. *J. Chem. Soc.* **1965**, *30*, 1148. (h) Cais, M.; Askhenazi, P.; Dani, S.; Gottlieb, J. *J. Organomet. Chem.* **1977**, *540*, 127. CpCo( $\eta^5$ -C<sub>7</sub>H<sub>5</sub>)<sub>2</sub>-radical: (i) Geiger, W. E.; Genneth, Th.; Lane, G. A. *Organometallics* **1986**, *5*, 1352. (propargyl radical)Co<sub>2</sub>(CO)<sub>6</sub>: (j) Padmanabhan, S.; Nicholas, K. M. *J. Organomet. Chem.* **1981**, *212*, 115.

(4) (a) Melikyan, G. G.; Vostrowsky, O.; Bauer, W.; Bestmann, H. J. *J. Organomet. Chem.* **1992**, *423*, C24. (b) Melikyan, G. G.; Combs, R. C.; Lamirand, J.; Khan, M.; Nicholas, K. M. *Tetrahedron Lett.* **1994**, 363. (c) Melikyan, G. G.; Deravakian, A. *J. Organomet. Chem.* **1997**, *544*, 143. (d) Melikyan, G. G.; Bright, S.; Monroe, T.; Hardcastle, K. M.; Ciurash, J. *Angew. Chem., Int. Ed.* **1998**, *37*, 161. (e) Melikyan, G. G.; Deravakian, A.; Myer, S.; Yadegar, S.; Hardcastle, K. I.; Ciurash, J.; Toure, P. *J. Organomet. Chem.* **1999**, *578*, 68. (f) Melikyan, G. G.; Sepanian, S.; Riahi, B.; Villena, F.; Jerome, J.; Ahrens, B.; McClain, R.; Matchett, J.; Scanlon, S.; Abrenica, E.; Paulsen, K.; Hardcastle, K. I. *J. Organomet. Chem.* **2003**, *683*, 324. (g) Melikyan, G. G.; Villena, F.; Sepanian, S.; Pulido, M.; Sarkissian, H.; Florut, A. *Org. Lett.* **2003**, *5*, 3395. (h) Melikyan, G. G.; Villena, F.; Florut, A.; Sepanian, S.; Sarkissian, H.; Rowe, A.; Toure, P.; Mehta, D.; Christian, N.; Myer, S.; Miller, D.; Scanlon, S.; Porazik, M. *Organometallics* **2006**, *25*, 4680.

highest stereoselectivity—with preponderant formation of *d,l*-diastereomers—was observed in THF-mediated and spontaneous dimerizations of  $\text{Co}_2(\text{CO})_6$ -complexed propargyl radicals (de 90–94%).<sup>4b–e</sup> To the contrary, *intermolecular radical cross-coupling reactions*, with an unpaired electron localized in an  $\alpha$ -position of a  $\pi$ -bonded ligand, remains practically unknown.<sup>2,3</sup> Conceptually related are radical dimerizations of  $\text{Fe}(\text{CO})_3$ -cyclohexadienyl complexes:<sup>3c,d</sup> the topology of a  $\pi$ -bonded ligand is such that the isomeric radicals can be generated at both ends of an unsaturated five-carbon moiety. Zinc-induced reduction of the monosubstituted cyclohexadienyl cation gave rise to isomeric 1,1- and 1,5-dimers (85:15; de 0%) with preponderant formation of sterically hindered head-to-head product.<sup>3c</sup> An electrochemical reduction of a 1,4-disubstituted analogue lacked both regio- and stereoselectivity.<sup>3d</sup> Our interest in this area stems from a systematic study on the chemistry of transition metal-templated propargyl radicals and cations<sup>4</sup> that led us to the discovery of the THF-mediated,<sup>4c,e,f</sup> and spontaneous,<sup>4g</sup> generation and coupling of  $\text{Co}_2(\text{CO})_6$ -coordinated propargyl radicals. It is noteworthy that the level of stereocontrol achieved in these reactions (up to 97% *d,l*-) remains unprecedented for intermolecular organometallic radical dimerizations.<sup>2,3</sup> Herewith we present the *first account on the chemo- and diastereoselectivity of the intermolecular radical cross-coupling reactions of cobalt-complexed propargyl radicals*. The current study was undertaken to determine to what extent the product distribution can be altered by varying the kinetic and thermodynamic parameters of the requisite cations and radicals.

## Results and Discussion

The current level of knowledge on stereoelectronic parameters of the  $\pi$ -bonded organometallic radicals is quite limited<sup>2,3,5</sup> and does not provide the reliable basis for predicting the chemo- and stereoselectivity of the reactions. The hybridization of the  $\alpha$ -radical center— $\text{sp}^2$  vs  $\text{sp}^3$ —and, attendant with it, the very shape of the immediate radical environment—planar vs pyramidal—remain unknown. For comparison, the respective oxidized species, the  $\text{Co}_2(\text{CO})_6$ -doubly-stabilized propargyl cation, is shown to maintain an  $\text{sp}^2$ -configuration with an  $\alpha$ -cationic center being shifted toward one of the cobalt atoms.<sup>4d</sup> Given the lack of literature precedence,<sup>2,3</sup> the chemo- and stereoselectivity of the intermolecular cross-coupling reactions is hard to predict. First, the “persistence” of carbon-based radicals<sup>6,7</sup> in the organometallic area is an unexplored category, even on a conceptual basis, and it remains to be understood how the cobalt-alkyne complex needs to be modified, at the core and at the periphery, in order to achieve a synthetically meaningful level of persistence. Second, using propargyl cations as precursors to the respective radicals adds a new variable, when compared to the purely organic environment,<sup>6,7</sup> which can also affect the product distribution.

(5) (a) Melikyan, G. G.; Nicholas, K. M. In *Modern Acetylene Chemistry*; Stang, P. J., Diederich, F., Eds.; VCH Publishers: Weinheim, 1995; Chapter 4. (b) McGlinchey, M. J.; Girard, L.; Ruffolo, R. *Coord. Chem Rev.* **1995**, *143*, 331. (c) Amouri, H. E.; Gruselle, M. *Chem. Rev.* **1996**, *96*, 1077. (d) Went, M. *Adv. Organomet. Chem.* **1997**, *41*, 69. (e) Green, J. R. *Curr. Org. Chem.* **2001**, *5*, 809. (f) Muller, T. J. J. *Eur. J. Org. Chem.* **2001**, 2021. (g) Teobald, B. J. *Tetrahedron* **2002**, *58*, 4133.

(6) (a) See: ref 1a, Chapter 4.1, p 758. (b) Griller, D.; Ingold, K. *Acc. Chem. Res.* **1976**, *9*, 13. (c) Fischer, H. *Chem. Rev.* **2001**, *101*, 3581, and references therein.

(7) (a) Fischer, H. *J. Am. Chem. Soc.* **1986**, *108*, 3925. (b) Allen, A. D.; Fenwick, M. F.; Riyad, H.; Tidwell, T. T. *J. Org. Chem.* **2001**, *66*, 5759. (c) Studer, A. *Chem.—Eur. J.* **2001**, *7*, 1159. (d) Alajarin, M.; Vidal, A.; Ortin, M.; Bautista, D. *New J. Chem.* **2004**, *28*, 570. (e) Wetter, C.; Jantos, K.; Woithe, K.; Studer, A. *Org. Lett.* **2003**, *5*, 2899.

Treatment of alcohols **1** and **2** with tetrafluoroboric acid<sup>5</sup> provided for concurrent generation of the cations **3** and **4** (Scheme 1). Their reduction with zinc (6-fold excess; 20 °C, 3 h) yielded propargyl radicals **5** and **6**, the key transient species previously employed in homo-coupling reactions.<sup>4b,e–g</sup> The concurrent homo- and cross-coupling reactions gave rise to respective dimeric products (**7**, **8**, and **9**) each represented by a mixture *d,l*- and *meso*-diastereomers. Three kinetic parameters need to be taken into consideration while considering the chemoselectivity of these reactions: (1) the rate of cation generation; (2) the rate of radical generation; and (3) the rate of dimerization itself. Since the two-step experimental protocol includes an isolation of the cations **3** and **4**, the alleged disparity in the rates of cation generation, caused by a *para*-substituent at the aromatic nucleus, becomes a noncontributing factor. The other two parameters, if nearly equal, should provide for a statistical product distribution.<sup>6,7</sup> By the NMR data, the ratio of dimers **7**:**8**:**9** in the crude mixture was equal to 22:40:38 (Table 1), which may be caused by either the faster generation of radical **6** or a higher rate of its self-dimerization, or the combination thereof. Given the fact that the *para*-methoxy group is remotely located from the reaction site, the assumption was made that the dimerization rate of radicals **5** and **6** cannot differ significantly. To examine if the charge distribution in cations **3** and **4** does, in fact, impact the reduction kinetics, semiempirical and *ab initio* studies<sup>8</sup> were carried out for cobalt-complexed cations **3** and **4** and their organic counterparts, **10** and **11** (Figure 1). For the former, as expected, a positive charge on the  $\alpha$ -carbon atom is higher than that in *p*-OMe derivative **11**, given the electron-donating nature of the substituent ( $C_1 +0.126233$  vs  $C_1 +0.042917$ ). The complexation, unexpectedly, reverses the trend and the positive charge in cation **3** becomes significantly lower when compared to that of cation **4** ( $C_1 +0.004863$  vs  $C_1 +0.382988$ ). A careful consideration of the computational data reveals more differences in the charge distribution caused by the interplay between an electron flow toward the cationic center and the intensity of the back-bonding between the transition metal and a  $\pi$ -bonded ligand. In particular, an electron donation from the *para*-substituent increases the negative charge on the aromatic carbon directly bonded to the cationic center (**3**  $C_{1'}$   $-0.086368$ ; **4**  $C_{1'}$   $-0.266173$ ), making the  $C_1$ – $C_{1'}$  bond more polar ( $\Delta\delta$  **3** 0.091231; **4** 0.649161) and also shorter ( $C_1$ – $C_{1'}$  **3** 1.464 Å, **4** 1.405 Å). Concurrently, the back-bonding decreases as indicated by an increased electron density over the cobalt atoms (**3**  $-0.404561$  and  $-0.421442$ ; **4**  $-0.472625$  and  $-0.479224$ ). Overall, the metal cluster acts as an electron reservoir by accommodating an additional electron density in response to an electronic shift from the *para*-substituent and toward the  $C_{1'}$  carbon atom. Most importantly, calculations revealed that an increased positive charge on the cationic  $C_1$  atom in cation **4** is, most probably, responsible for the nonstatistical product distribution in the zinc-mediated reaction.

The level of diastereoselection is comparable in homo- and cross-dimeric products (Scheme 1; de 66–76%) with preponderant formation of *d,l*-stereoisomers (*d,l*:*meso*: **7** 83:17; **8** 88:12; **9** 88:12). Stereochemical assignments are based on the X-ray crystallography data<sup>4b,f</sup> and NMR signatures of methyne protons.<sup>4c,f,g</sup> Given the complexity of the mixture, the isolation of the individual stereoisomers was carried out, by preparative TLC, in three steps, with no significant changes in the stereoisomeric compositions (*d,l*:*meso*: **7** 87:13; **8** 82:18; **9** 88:12). Depicted in Figures 2 and 3 are staggered orientations of

(8) Titan; Wavefunction, Inc. All geometries were optimized at the PM3 and 3-21G\* levels, 2000.

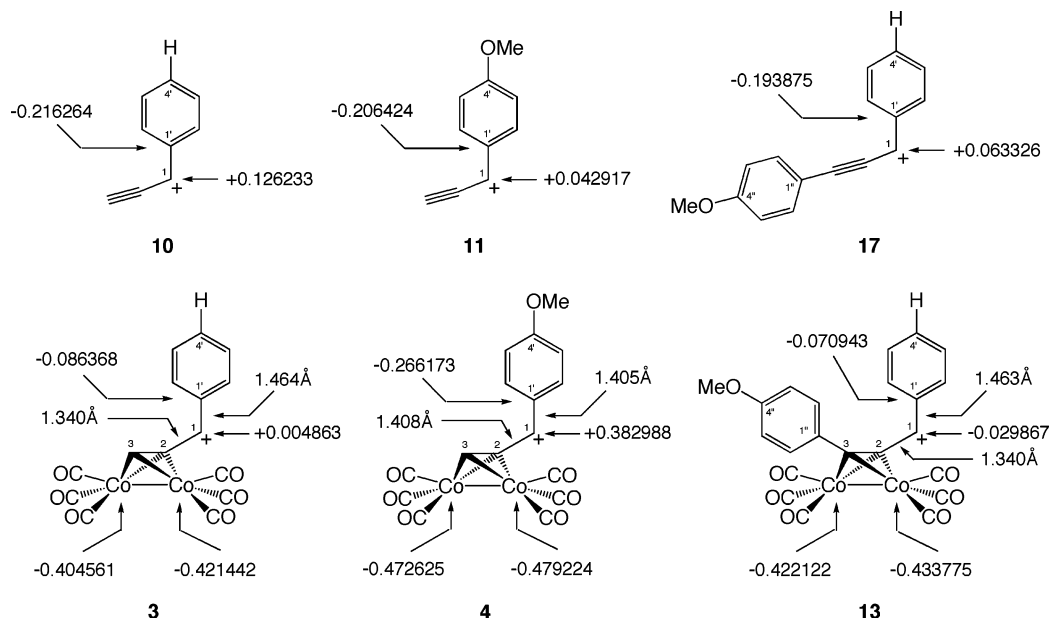
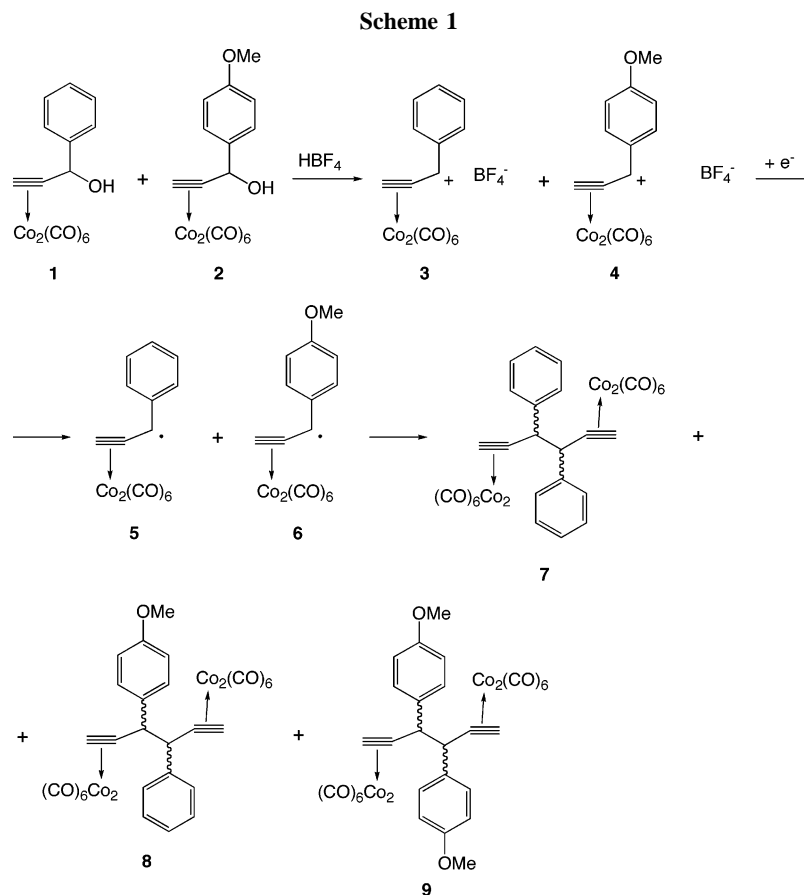
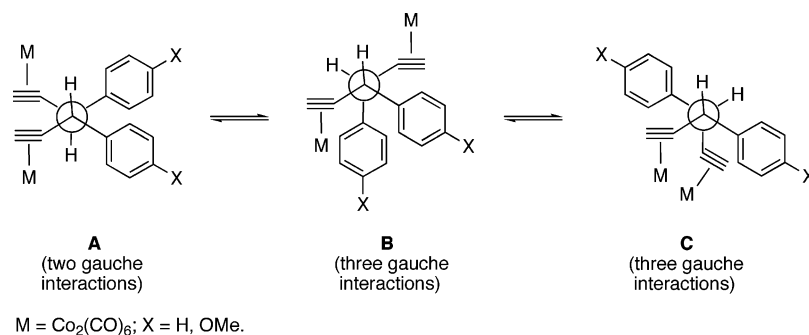


Figure 1. Charge distribution and structural parameters derived from the PM3 (3, 4, 13) and 3-21G\* (10, 11, 17) calculations.



converging propargyl radicals prior to the formation of *d,l*- and *meso*-stereoisomers, respectively. For each diastereomer, there are three staggered orientations (A–F) differing in the number of supposedly destabilizing *gauche* interactions (two vs three). For *d,l*-diastereomers, the most favorable orientation is represented by the structure A, with two *gauche* interactions, as opposed to the alternative orientations B and C, each featuring three *gauche* interactions (Figure 2). It is worthy to mention that the X-ray crystallography for *d,l*-diastereomer 9<sup>4f</sup> proves

that an orientation A is energetically most feasible with pairs of cobalt-alkyne units and aromatic rings opposed to each other. Among the three orientations that could give rise to *meso*-diastereomers—D, E, and F—the former two are less favorable, each featuring three *gauche* interactions (Figure 3). To interpret the observed preponderant formation of *d,l*-stereoisomers 7–9, one has to compare orientations A and F, each having only two *gauche* interactions. The assumption needs to be made that the repulsion between two cobalt-alkyne units and two aromatic



**Figure 2.** Formation of *d,l*-diastereomers **7–9**: staggered orientations of converging propargyl radicals.

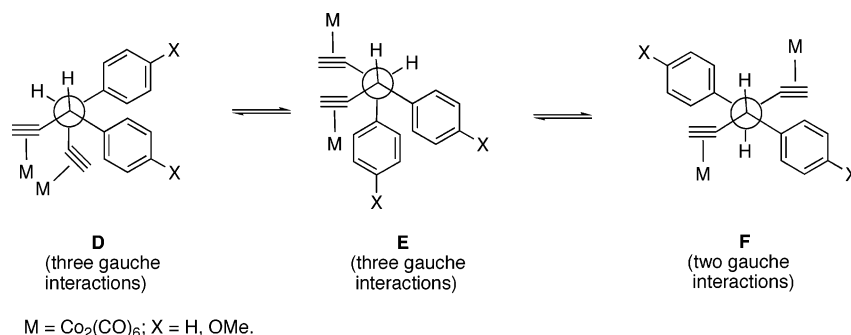


**Figure 3.** Formation of *meso*-diastereomers **7–9**: staggered orientations of converging propargyl radicals.

**Table 1. Chemo- and Diastereoselectivity of Radical Cross-Coupling Reactions**

reduction method	<b>7</b>		<b>8</b>		<b>9</b>	
	<i>d,l</i> + <i>meso</i>	<i>d,l</i> : <i>meso</i>	<i>d,l</i> + <i>meso</i>	<i>d,l</i> : <i>meso</i>	<i>d,l</i> + <i>meso</i>	<i>d,l</i> : <i>meso</i>
1. Zn	22	83:17	40	88:12	38	88:12
2. Cp <sub>2</sub> Co	33	78:22	38	70:30	29	75:25
3. THF-mediated, one-step coupling protocol <sup>4h</sup>	26	92:8	49	94:6	25	95:5
4. Tf <sub>2</sub> O-mediated, one-step coupling protocol <sup>4g</sup>	19	88:12	47	94:6	34	96:4

rings in **A** is significantly less than that of two pairs of cobalt-alkyne units and aromatic rings in **F**. To what extent an alleged  $\pi$ -stacking between aromatic rings could provide for an additional stabilization remains unclear.

Replacement of zinc, a heterogeneous reducing agent, with cobaltocene, a 19e<sup>-</sup> homogeneous reducing agent, substantially changes the reaction profile. The latter is a relatively bulky molecule (199.56 Å<sup>3</sup>) comparable in volume with that of starting alcohols (**1** 327.60 Å<sup>3</sup>; **2** 362.18 Å<sup>3</sup>). The rate of the radical generation will then be dependent upon the ability of cobaltocene to approach the cationic center to effectively overlap a donor orbital with a p-orbital of the cation, which, in turn, is interacting, through-space, with an electron-rich cobalt cluster.<sup>4d</sup> By the NMR data, the ratio of dimers **7**:**8**:**9** in the crude mixture was equal to 33:38:29 (Table 1). While the concentration of the cross-dimer **8** remains nearly the same (Zn 40%; Cp<sub>2</sub>Co 38%), the homo-dimers **7** and **9** are formed in almost equal quantities (33%; 29%). It is indicative of the stronger reducing power of cobaltocene, as opposed to that of zinc, which does not allow for the discrimination of the requisite cations **3** and **4** based on the electrophilicity of the cationic center. The stereoselectivity of the cobaltocene-mediated reaction (Table 1, entry 2) is systematically lower (de 40–56%) revealing a nontrivial dependence of the stereochemical outcome of the radical coupling reaction on the nature of the reducing agent. From a theoretical standpoint, one could expect the stereoselectivity of the coupling of *free radicals* to be independent of the radical generation mode. Its observed dependency (Table

1) is indicative of the contribution made to the assembly of the converging radicals by an oxidized form of cobaltocene (radical-ion pair).

The THF-mediated, one-step dimerization protocol<sup>4h</sup> (Table 1, entry 3) includes the treatment of equimolar amounts of alcohols **1** and **2** with a 2-fold excess of THF and HBF<sub>4</sub>. The reaction introduces another variable, cation generation rate, since a one-step procedure does not involve isolation of the requisite cations **3** and **4**. A nearly statistical distribution was observed for radical coupling products (**7**:**8**:**9**, 26:49:25), along with a higher *d,l*-diastereoselectivity of 92–95% (de 84–90%). The THF-mediated reaction has a complex multistep mechanism<sup>4h</sup> that involves coordination of two molecules of THF with a cationic center and the consecutive cluster-to-cluster reduction between electronically unequal metal cores and cluster-to-ligand electron transfer, with the latter actually generating radicals **5** and **6**. The reaction is known to provide for a better selectivity in intermolecular dimerization reactions: a ratio of *d,l*:*meso* diastereomers of **7** is equal to 75:25<sup>4b</sup> and 95:5<sup>4d</sup> in Zn- and THF-mediated reactions, respectively. The *spontaneous radical generation reaction* mediated by triflic anhydride<sup>4g</sup> yielded 47% of cross-dimer **8**; distribution of homo-dimers **7** and **9** significantly deviated from the statistical distribution with the preponderant formation of the latter (**7**:**9**, 19:34; Table 1, entry 4). The mechanism of the reaction includes an instantaneous formation of mixed esters when requisite alcohols are treated with Tf<sub>2</sub>O, followed by a slow heterolysis of the  $\alpha$ -C–O bond and an *in situ* generation of the cations **3** and **4**.<sup>4g</sup> The level of observed stereoselectivity is comparable to that of the

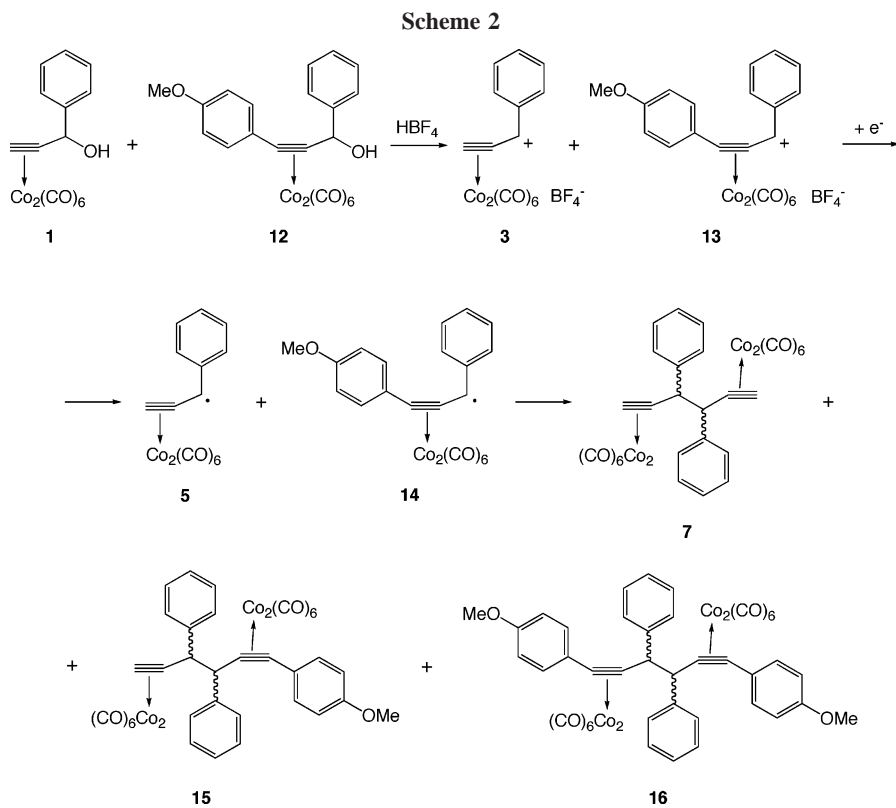


**Table 2. Chemo- and Diastereoselectivity of Radical Cross-Coupling Reactions<sup>a,b</sup>**

reduction method	molar ratios 1:12	7		15		16	
		<i>d,l</i> + <i>meso</i>	<i>d,l</i> : <i>meso</i>	<i>d,l</i> + <i>meso</i>	<i>d,l</i> : <i>meso</i>	<i>d,l</i> + <i>meso</i>	<i>d,l</i> : <i>meso</i>
1. Zn	1:1	39(25)	85:15	16(50)	74:26	45(25)	72:28
2. Zn	2:1	52(45)	78:22	24(44)	70:30	24(11)	70:30
3. Zn	3:1	63(56)	83:17	21(38)	72:28	17(6)	67:33
4. Zn	7:1	83(76)	85:15	8(22)	71:29	9(2)	67:33
5. Zn	9:1	86(81)	86:14	8(18)	71:29	6(1)	67:33
6. Zn	1:3	17(6)	79:21	23(38)	70:30	60(56)	72:28
7. Cp <sub>2</sub> Co	1:1	47(25)	76:24	47(50)	70:30	6(25)	57:43
8. THF	1:1	53(25)	92:8	14(50)	86:14	33(25)	82:18

<sup>a</sup> Product distribution and diastereomeric ratios are determined by NMR. <sup>b</sup> Statistical distribution is shown in parentheses.

THF-mediated reaction (*d,l*:*meso*, **8** 94:6; **9** 96:4), with a slight decrease for homo-dimer **7** (*d,l*:*meso*, 88:12 vs 92:8). The observed disparity in product distribution and a level of diastereocontrol allows us to conclude that the substrate structure and radical generation algorithm are the most critical parameters of the reaction, and the cross-coupling product is best formed, and with a highest diastereoselectivity, in THF- and Tf<sub>2</sub>O-mediated reactions, with Zn and Cp<sub>2</sub>Co being inferior by both criteria chosen.

The impact of the  $\gamma$ -aryl group upon chemo- and diastereoselectivity was then studied by employing the alcohol **12**, along with parent alcohol **1**, as a second component of the cross-coupling reaction (Scheme 2). The rationale behind this was that the presence of the bulky aromatic ring, in tandem with a bent geometry of the triple bond,<sup>5</sup> can make radical **14** more persistent,<sup>6,7</sup> thus retarding the rate of the homo-coupling reaction and, to the contrary, facilitating the formation of the cross-coupling product **15**. Another outcome could have been *not steric, but an electronic impact of the  $\gamma$ -arylmethoxy group* that could affect the electrophilicity of the cation **13**, thus creating a precondition for a *kinetic differentiation at the radical generation step*. The treatment of propargyl alcohols **1** and **12**, in a molar ratio 1:1, with an excess of HBF<sub>4</sub> yielded respective

cations **3** and **13**, which, upon isolation, were treated with zinc to produce propargyl radicals **5** and **14**. The subsequent radical coupling afforded the mixture of homo- and cross-dimers **7**:**15**:**16** in the ratio 39:16:45 (Table 2, entry 1). These data represent a significant departure from a nearly statistical distribution of the products observed in the absence of a substituent in the  $\gamma$ -position of propargyl alcohol (Table 1; cross-dimer **8** 38–47%). In fact, a dramatic drop in the concentration of the cross-product **15** points to a substantial difference in the generation rate of prerequisite radicals **5** and **14**. Most probably, because of the electronic differences and charge distribution in cations **3** and **13**, their reduction is well separated in time with one of them (**3**) being reduced at a much higher rate. To interpret these data, semiempirical and *ab initio* studies<sup>8</sup> were carried out for cobalt-complexed cations **3** and **13** and their organic counterparts **10** and **17** (Figure 1). For the latter, the electropositivity of the C<sub>1</sub> atom is much lower when compared to that in the parent cation **10** (**17** C<sub>1</sub> +0.063326; **10** C<sub>1</sub> +0.126233) (Figure 1), a difference that should be attributed to the donating properties of a 4'-OMeC<sub>6</sub>H<sub>4</sub> substituent. The same trend is noticeable in cobalt-complexed cations **3** and **13**: for the former, the central carbon atom (C<sub>1</sub>) is nearly electroneutral (C<sub>1</sub> +0.004863), while in the latter the cationic center acquires a partial negative charge

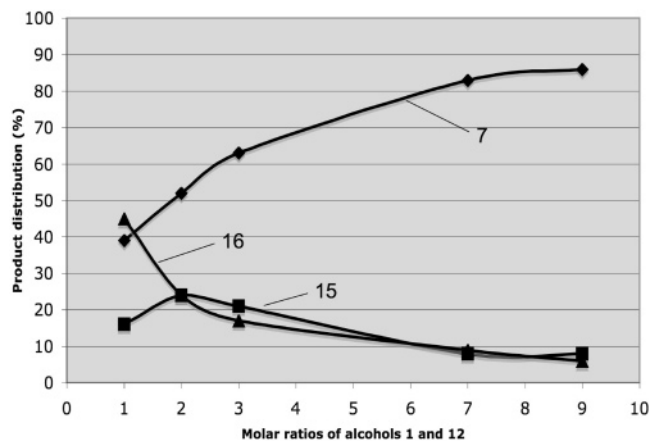


**Figure 4.** Product distribution as a function of a molar ratio of alcohols **1** and **12**.

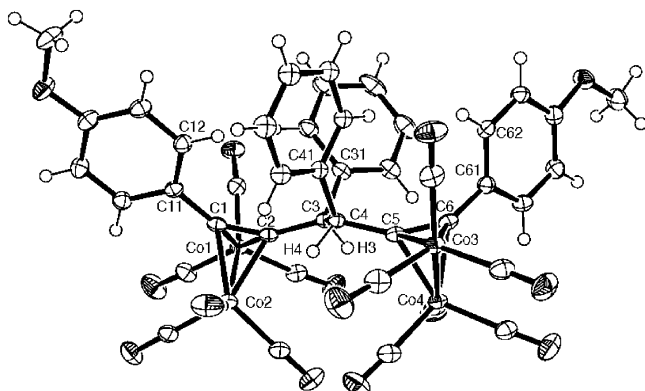


**Figure 5.** ORTEP diagram of the molecular structure of complex *d,l*-**16** with 30% probability ellipsoids.

( $C_1 - 0.029867$ )! The calculation data also indicate that the geometric and electronic parameters in close vicinity to the cationic center remain nearly identical (Figure 1;  $C_1$  **3**  $-0.086368$ , **13**  $-0.070943$ ;  $C_1 - C_1$  **3**  $1.464 \text{ \AA}$ , **13**  $1.463 \text{ \AA}$ ;  $C_1 - C_2$  **3**  $1.340 \text{ \AA}$ , **13**  $1.340 \text{ \AA}$ ), while a donation from a 4'-OMeC<sub>6</sub>H<sub>4</sub> substituent increases the electron density over the metal core (**3** Co  $-0.404561$ ;  $-0.421442$ ; **13**  $-0.422122$ ;  $-0.433775$ ).

On the basis of the calculation data, the observed chemoselectivity (**7**:**15**:**16**, 39:16:45; Table 2, entry 1) can be accounted for in terms of kinetic differentiation at the radical generation step: cation **3** is reduced at a higher rate than its counterpart **13** because in the latter the central carbon atom ( $C_1$ ) is less receptive toward an electron transfer from a reducing agent (Figure 1:  $C_1$  **3**  $+0.004863$ , **13**  $-0.029867$ ). The low concentration of the cross-dimer **15** (16%) is indicative of the disparity in the generation of the respective radicals, **5** and **14**. To establish if the product distribution can be modified by using, as a tool, the molar ratio of alcohols **1** and **12**, the latter was varied from 1:1 to 9:1 and the ratio of products and their diastereoselectivity were determined by NMR (Table 2, entries 2–5; Figure 4). The percentage of homo-dimer **7** gradually increased (from 39% to 86%), while the formation of its counterpart, **16**, dropped significantly (from 45% to 6%). The formation of cross-product **15** was most favorable at the ratio of **1**:**12** equal to 2:1 (24%; Table 2, entry 2), undergoing a gradual decline with further increase in the molar ratio of the starting alcohols. Also presented in Table 2, in parentheses, are the statistical ratios of products **7**, **15**, and **16**. Homo-dimers **7** and **16** are formed in higher quantities than statistically expected, independent from the molar ratio of starting alcohols **1** and **12**.

**Table 3.** Summary of the Crystal Structure Data for Complex *d,l*-**16**

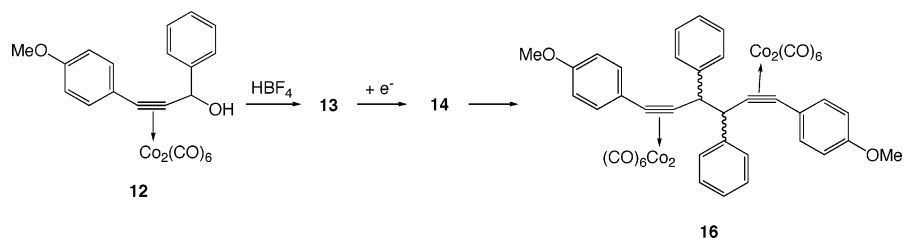
formula	C <sub>47</sub> H <sub>26</sub> O <sub>15</sub> Co <sub>4</sub>
fw	1066.40
temperature, K	100(2)
cryst color	dark red
cryst dimens, mm	0.308 × 0.300 × 0.092
cryst syst	triclinic
<i>a</i> , Å	11.0937(8)
<i>b</i> , Å	13.5833(10)
<i>c</i> , Å	17.9283(12)
$\alpha$ , deg	69.733(6)
$\beta$ , deg	71.212(6)
$\gamma$ , deg	66.574(7)
volume, Å <sup>3</sup>	2271.5(3)
space group	<i>P1</i>
<i>Z</i>	2
<i>D</i> (calc), Mg/m <sup>3</sup>	1.559
$\mu$ (Mo K $\alpha$ ), mm <sup>-1</sup>	1.504
no. of indep reflns	10 063 [ <i>R</i> <sub>i</sub> = 0.0538]
absorp corr	none
no. of data/restraints/params	10 063/0/575
goodness-of-fit on <i>F</i> <sup>2</sup>	1.157
final <i>R</i> indices [ <i>I</i> > 2 $\sigma$ ( <i>I</i> )]	
<i>R</i> 1	0.0495
w <i>R</i> 2	0.1232
largest diff peak, hole, e Å <sup>-3</sup>	1.223, $-0.576$

To the contrary, the observed amounts of the cross-product **15** are systematically lower than those theoretically anticipated, with the numerical data converging with an increase in the molar ratio of reactants (Table 2: **1**:**12** 1:1, **15** 16% vs 50%; 9:1, 8% vs 18%). Using a larger excess of alcohol **12** (Table 2, entries 3 and 6) resulted in a reversal in the concentration of homo-dimers **7** and **16**, while the amount of cross-product **15** remained nearly the same (21% vs 23%). A rather dramatic change in chemoselectivity was observed in the case of Cp<sub>2</sub>Co, acting as a reducing agent (Table 2). The concentration of the cross-dimer **15** reaches the highest mark (47%), while the formation of the homo-dimer **16** suffers a significant decline (6%). In the THF-mediated reaction, the product distribution is strikingly different (**7**:**15**:**16**, 53:14:33) from a nearly statistical distribution observed in the case of propargyl alcohols with terminal triple bonds (Table 1: **7**:**8**:**9**, 26:49:25). One of the contributing factors in a one-step, THF-mediated reaction is the rate of cation generation since the latter is converted to the respective radicals *in situ*, without their isolation in an individual form.

The diastereoselectivity data are summarized in Table 2. Stereochemical assignments for dimers **7** and **15** are based on the X-ray crystallography data<sup>4b,f</sup> and NMR signatures of methyne protons.<sup>4c,f,g</sup> In the case of homo-dimer **16**, the NMR data were not sufficient for an unambiguous stereochemical assignment and the structure of the major stereoisomer, as *d,l*-**16**, was determined by X-ray crystallography (Figure 5).<sup>9</sup> The synthesis was carried out by the treatment of cation **13** with a 6-fold excess of zinc at ambient temperature and isolation of the homo-dimer as a mixture of *d,l*:*meso*, 93:7 (Scheme 3). From the conformational point of view, *d,l*-**16** appears to substantially differ from bis-cobalt complexes with *terminal triple bonds*.<sup>4b,e,f</sup> The latter arrange both acetylenic moieties in close proximity to each other, while phenyl<sup>4b,f</sup> or methyl<sup>4e</sup> groups are oriented *gauche*, with a different degree of conformational distortion (44–46°). Consequently, the internal hydrogen atoms (H<sub>3A</sub> and H<sub>4A</sub>) are disposed *anti* to each other (171–172°).<sup>4e,f</sup> In *d,l*-**16**, given the presence of bulky  $\gamma$ -phenyl substituents, the alkyne

(9) (a) Oxford Diffraction. *Crystalis CCD and RED*, Version 1.70; Oxford Diffraction Ltd.: Oxford, UK, 2002. (b) Sheldrick, G. M. *SHELX-97*, Program for the Solution and Refinement of Crystal Structures, University of Göttingen: Göttingen, Germany, 1997.

Scheme 3

Table 4. Selected Bond Lengths (Å) and Bond and Torsion Angles (deg) for Complex *d,l*-16

Bond Lengths			
Co(1)–Co(2)	2.464(5)	Co(3)–Co(4)	2.469(5)
Co(1)–C(1)	1.995(3)	Co(3)–C(5)	1.969(3)
Co(1)–C(2)	1.986(2)	Co(3)–C(6)	1.996(3)
C(1)–C(2)	1.344(4)	C(5)–C(6)	1.341(4)
Co(2)–C(1)	1.980(2)	Co(4)–C(5)	1.976(2)
Co(2)–C(2)	1.983(2)	Co(4)–C(6)	1.970(2)
Bond Angles			
C(11)–C(1)–C(2)	147.3(2)	C(1)–C(2)–C(3)	150.1(2)
C(4)–C(5)–C(6)	148.7(2)	C(5)–C(6)–C(61)	146.1(2)
Dihedral Angles			
C(1)–C(2)–C(3)–C(31)	99.0	C(1)–C(2)–C(3)–C(4)	65.8
C(2)–C(3)–C(4)–C(5)	150.5	C(41)–C(4)–C(3)–C(31)	48.2
H(3)–C(3)–C(4)–H(4)	81.6	C(11)–C(1)–C(2)–C(3)	3.6
C(61)–C(6)–C(5)–C(4)	0.6	C(41)–C(4)–C(3)–H(3)	162.7
C(5)–C(4)–C(3)–C(31)	79.6	C(41)–C(4)–C(3)–C(2)	81.7
H(4)–C(4)–C(3)–C(2)	34.1	H(4)–C(4)–C(3)–C(31)	164.0°
Co(1)–Co(2)–C(1)–C(2)	73.6	Co(3)–Co(4)–C(5)–C(6)	74.4°
C(2)–C(1)–C(11)–C(12)	1.2	C(5)–C(6)–C(61)–C(62)	127.3°

units are pushed apart from each other, representing an *anti* conformation around an internal C<sub>3</sub>–C<sub>4</sub> bond (C<sub>2</sub>–C<sub>3</sub>–C<sub>4</sub>–C<sub>5</sub> 150.5°). Hydrogen atoms attached to the asymmetric centers (H<sub>3</sub>, H<sub>4</sub>) are located *gauche* to each other (H<sub>3</sub>–C<sub>3</sub>–C<sub>4</sub>–H<sub>4</sub> 81.6°), as are the unsubstituted phenyl groups (C<sub>31</sub>–C<sub>3</sub>–C<sub>4</sub>–C<sub>41</sub> 48.2°). Metal cores Co<sub>2</sub>C<sub>2</sub> represent tetrahedrons with a skew geometry where the angles between Co–Co and C–C triple bonds are significantly deviated from the perpendicular arrangement (73.6°; 74.4°).<sup>5a</sup> Spatially, the  $\gamma$ -phenyl groups are not equivalent and are positioned differently with respect to the triple bonds: one of the phenyl groups is located in the plane of the triple bond [C(2)–C(1)–C(11)–C(12) 1.2°], while the other exhibits a significant twist [C(5)–C(6)–C(61)–C(62) 127.3°]. Other noteworthy structural features of *d,l*-16 include (a) an essentially undistorted planarity of alkyne moieties (C<sub>11</sub>–C<sub>1</sub>–C<sub>2</sub>–C<sub>3</sub> 3.6°, C<sub>61</sub>–C<sub>6</sub>–C<sub>5</sub>–C<sub>4</sub> 0.6°); (b) a bent geometry<sup>5,10</sup> for coordinated alkyne units (C<sub>11</sub>–C<sub>1</sub>–C<sub>2</sub> 147.3°, C<sub>1</sub>–C<sub>2</sub>–C<sub>3</sub> 150.1°, C<sub>4</sub>–C<sub>5</sub>–C<sub>6</sub> 148.7°, C<sub>5</sub>–C<sub>6</sub>–C<sub>61</sub> 146.1°), reflecting substantial rehybridization of and strong back-bonding to the alkyne from the cobalt carbonyl moiety; and (c) a lengthened coordinated C–C triple bond (1.34 Å vs ca. 1.21 Å for free ligand) attendant with complexation to the transition metal.

The level of diastereoselection for *d,l*- and *meso*-7 varies in a wide range, from 76:24 to 92:8 (Table 2), with preponderant formation of the *d,l*-stereoisomer for all reducing agents and alternative experimental protocols studied so far. The lowest stereoselectivity is observed in the case of Cp<sub>2</sub>Co (de 52%), while the highest level of stereoselection was reported in the THF-mediated process (de 84%). The stereoselectivity is systematically lower for the homo-dimer 16, containing a  $\gamma$ -phenyl substituent at the triple bond: *d,l:meso* ratio varies from 57:43 to 82:18. Curiously, both extremes are again observed in the case of Cp<sub>2</sub>Co (de 14%) and the THF-mediated

process (de 64%). The same phenomenon was observed for cross-dimer 15: Cp<sub>2</sub>Co *d,l:meso*, 70:30; THF *d,l:meso*, 86:14. Careful analysis of *d,l:meso* ratios (Table 2) revealed another tendency that cannot be easily interpreted: for nearly every reported case, the *d,l*-diastereoselectivity of cross-dimer 15 is lower than that for homo-dimer 7 and higher than that for homo-dimer 16.

*d,l*-3,4-Diaryl-1,5-alkadiynes are not easily accessible by alternative means.<sup>11</sup> The “classical” propargyl–propargyl coupling reaction<sup>11a</sup> is accompanied by acetylene–allene rearrangement and, attendant with it, a poor regioselectivity. Mixtures of three isomeric compounds are usually formed—*head-to-head*, *head-to-tail*, and *tail-to-tail*—with their separation being a difficult experimental task.<sup>11a</sup> *d,l*-3,4-Diaryl-1,5-hexadiynes are produced in a ruthenium-catalyzed process,<sup>11b</sup> although the reaction is inherently limited in scope, and both yields and diastereoselectivities drastically decrease with either electron-withdrawing (CF<sub>3</sub>) or electron-donating substituents (Me; OMe) introduced to the aromatic nuclei. The reproducibility of the experimental data might also be problematic since the authors claim the presence of “...adventitious molecular oxygen...” to be essential to the mechanism of the reaction.<sup>11b</sup> Intermolecular coupling of propargyl alcohols can also be mediated by a Ti-(OiPr)<sub>2</sub>Cl<sub>2</sub>/Mg mixture,<sup>11c</sup> although the process, from the synthetic point of view, remains highly deficient: (a) in the case of propargyl alcohols with a terminal triple bond, target 1,5-alkadiynes are accompanied by comparable quantities of acetylenic allenes (45–50%), which are difficult to separate; (b) the reaction lacks diastereoselectivity and suffers from low conversions (70–72%); and (c) the isolation of the products in a homogeneous form is not achievable.<sup>11c</sup> Palladium-catalyzed

(11) (a) Badanyan, Sh. O.; Voskanyan, M. G.; Chobanyan, Zh. A. *Russ. Chem. Rev.* **1981**, *50*, 1074. (b) Onodera G.; Nishibayashi, Y.; Uemura, S. *Organometallics* **2006**, *25*, 35. (c) Yang, F.; Zhao, G.; Ding, Y.; Zhao, Z.; Zheng, Y. *Tetrahedron Lett.* **2002**, *43*, 1289. (d) Ogoshi, S.; Nishiguchi, S.; Tsutsumi, K.; Kurosawa, H. *J. Org. Chem.* **1995**, *60*, 4650.

(10) Dickson, R. S.; Fraser, P. J. *Advances in Organometallic Chemistry* **12**; Academic Press: New York, 1974; p 323.

reductive homo-coupling reaction of propargyl carbonates yields unsubstituted 1,5-alkadiynes as minor products (5–29%), along with isomeric allene-ynes.<sup>11d</sup>

### Conclusion

Chemo- and diastereoselectivities of homo- and cross-coupling reactions of  $\text{Co}_2(\text{CO})_6$ -complexed propargyl radicals are dependent upon the structural and electronic parameters of the substrates. Among alternative radical generation methods—reduction of respective cations with Zn or  $\text{Cp}_2\text{Co}$  and one-step mediation with THF or  $\text{Tf}_2\text{O}$ —the latter two provided for the highest level of *d,l*-diastereocontrol (de up to 92%). A donating, and bulky,  $\gamma$ -aromatic ring did not increase the *persistence* of the propargyl radicals, but caused the *kinetic differentiation* at the radical generation step and nonstatistical distribution of the dimeric products. The chemoselectivity (the ratio of homo- and cross-coupling products) is consistent with the computational data: the electrophilicity of the  $\alpha$ -cationic center is unexpectedly enhanced by a *p*-methoxy substituent at the  $\alpha$ -phenyl group and, to the contrary, is decreased due to the presence of the  $\gamma$ -aromatic ring.

### Experimental Section

All manipulations of air-sensitive materials were carried out in flame-dried Schlenk-type glassware on a dual-manifold Schlenk line interfaced to a vacuum line. Argon and nitrogen (Airgas, ultrahigh purity) were dried by passing through a Drierite tube (Hammond). All solvents were distilled before use under dry nitrogen over appropriate drying agents (ether, THF, from sodium benzophenone ketyl;  $\text{CH}_2\text{Cl}_2$ , from  $\text{CaH}_2$ ; benzene, from sodium). All reagents were purchased from Sigma-Aldrich and used as received.  $\text{Co}_2(\text{CO})_8$  was purchased from Strem. NMR solvents were supplied by Cambridge Isotope Laboratories.  $^1\text{H}$  and  $^{13}\text{C}$  NMR spectra were recorded on a Bruker DRX-400 ( $^1\text{H}$ , 400 MHz) spectrometer. Chemical shifts were referenced to internal solvent resonances and are reported relative to tetramethylsilane. Spin-spin coupling constants (*J*) are given in hertz. Elemental analyses were performed by Desert Analytics (Tucson, AZ). Melting temperatures (uncorrected) were measured on a Mel-Temp II (Laboratory Devices) apparatus. Silica gel S733-1 (200–425 mesh; Fisher) was used for flash column chromatography. Analytical and preparative TLC analyses were conducted on silica gel 60 F<sub>254</sub> (EM Science; aluminum sheets) and silica gel 60 PF<sub>254</sub> (EM Science; w/gypsum), respectively. Eluents are ether (E), petroleum ether (PE), and benzene (B). Mass spectra were run at the Regional Center on Mass-Spectroscopy, UC Riverside, Riverside, CA (FAB, ZAB-SE;  $\text{CI-NH}_3$ , 7070EHF; Micromass).

***d,l*- and meso-(3,4-Diphenyl-1,5-hexadiyne)bis(dicobalthexacarbonyl) (7), *d,l*- and meso-[3-(4'-Methoxyphenyl)-4-phenyl-1,5-hexadiyne]bis(dicobalthexacarbonyl) (8), and *d,l*- and meso-[3,4-Di(4'-methoxyphenyl)-1,5-hexadiyne]bis(dicobalthexacarbonyl) (9).** **Reduction with Zinc.** Under an atmosphere of nitrogen,  $\text{HBF}_4\cdot\text{Me}_2\text{O}$  (201 mg, 1.50 mmol) was added dropwise to a solution of alcohol **1** (52 mg, 0.125 mmol) and alcohol **2** (56 mg, 0.125 mmol) in dry ether (20 mL) at  $-20^\circ\text{C}$ . The reaction mixture was stirred for 1 h, and the ethereal layer was removed. At  $-20^\circ\text{C}$ , the cations **3** and **4** were washed with dry ether ( $2 \times 15$  mL), the residual solvent was removed under reduced pressure, and the precipitate was dissolved in dry  $\text{CH}_2\text{Cl}_2$  (5 mL). The reaction mixture was then treated with zinc (98 mg, 1.5 mmol) and stirred at  $20^\circ\text{C}$  for 3 h (TLC control). Zinc was filtered off, and the crude mixture was examined by NMR (*d,l*-7:*meso*-7, 83:17; *d,l*-8:*meso*-8, 88:12; *d,l*-9:*meso*-9, 88:12; **7:8:9**, 22:40:38) and fractionated on preparative TLC plates (silica gel,  $20 \times 20$  cm). Step 1 (PE:E, 20:1; 3 plates): fraction 1 *d,l*-7, *meso*-7, and *meso*-

**8**; fraction 2 *d,l*-8 and *meso*-9; fraction 3 *d,l*-9. Step 2, reseparation of fraction 1 (PE; 2 plates): *d,l*-7 and *meso*-7 (combined) and *meso*-8. Step 3, reseparation of fraction 2 (PE: $\text{C}_6\text{H}_6$ , 7:1; 1 plate): *d,l*-8 and *meso*-9.

*d,l*- and *meso*-7: 12.5 mg was obtained (25.0%). By NMR, the *d,l*:*meso* ratio was equal to 87:13, de 74%. Spectral and physicochemical characteristics are identical with those reported earlier.<sup>4h</sup>

*meso*-8: 3.9 mg was obtained (3.8%); dark red oil. TLC (PE:E, 2:1):  $R_f$  0.60.  $^1\text{H}$  NMR (400 MHz,  $\text{CDCl}_3$ ):  $\delta$  3.89 (3H, s,  $\text{OCH}_3$ ), 4.38 (2H, AB-spectrum, CH,  $J = 12.0$ ), 4.96 (1H, s,  $\text{HC}\equiv$ ), 5.06 (1H, s,  $\text{HC}\equiv$ ), 6.90–7.55 (9H, m, aromatic H). MS-FAB:  $m/z$  748 ( $\text{M}^+ - 3\text{CO}$ ), 663 ( $\text{M}^+ - 6\text{CO} - \text{H}$ ), 635 ( $\text{M}^+ - 7\text{CO} - \text{H}$ ), 607 ( $\text{M}^+ - 8\text{CO} - \text{H}$ ), 579 ( $\text{M}^+ - 9\text{CO} - \text{H}$ ), 551 ( $\text{M}^+ - 10\text{CO} - \text{H}$ ), 524 ( $\text{M}^+ - 11\text{CO}$ ), 378 ( $\text{M}^+ - 12\text{CO} - 2\text{Co}$ ). *d,l*-8: 18.0 mg was obtained (17.5%). The ratio of *d,l*-8:*meso*-8 was equal to 82:18 (by weight), de 64%; dark red crystals;  $T_{\text{dec}} 75\text{--}115^\circ\text{C}$  (sealed capillary; coevaporated with benzene,  $3 \times 1$  mL). TLC (PE:E, 2:1):  $R_f$  0.54.  $^1\text{H}$  NMR (400 MHz,  $\text{CDCl}_3$ ):  $\delta$  3.69 (3H, s,  $\text{OCH}_3$ ), 4.33 (2H, s, CH), 6.31 (2H, d,  $\text{HC}\equiv$ ,  $J = 1.4$ ), 6.69 (2H, d, aromatic H,  $J = 8.5$ ), 7.03 (2H, d, aromatic H), 7.13 (5H, m, aromatic H). MS-FAB:  $m/z$  748 ( $\text{M}^+ - 3\text{CO}$ ), 720 ( $\text{M}^+ - 4\text{CO}$ ), 691 ( $\text{M}^+ - 5\text{CO} - \text{H}$ ), 664 ( $\text{M}^+ - 6\text{CO}$ ), 663 ( $\text{M}^+ - 6\text{CO} - \text{H}$ ), 636 ( $\text{M}^+ - 7\text{CO}$ ), 635 ( $\text{M}^+ - 7\text{CO} - \text{H}$ ), 608 ( $\text{M}^+ - 8\text{CO}$ ), 607 ( $\text{M}^+ - 8\text{CO} - \text{H}$ ), 580 ( $\text{M}^+ - 9\text{CO}$ ), 579 ( $\text{M}^+ - 9\text{CO} - \text{H}$ ), 552 ( $\text{M}^+ - 10\text{CO}$ ), 551 ( $\text{M}^+ - 10\text{CO} - \text{H}$ ), 523 ( $\text{M}^+ - 11\text{CO} - \text{H}$ ), 495 ( $\text{M}^+ - 12\text{CO} - \text{H}$ ), 437 ( $\text{M}^+ - 12\text{CO} - \text{Co} - \text{H}$ ), 378 ( $\text{M}^+ - 12\text{CO} - 2\text{Co}$ ), 319 ( $\text{M}^+ - 12\text{CO} - 3\text{Co} - \text{H}$ ). Anal. Calcd for  $\text{C}_{31}\text{H}_{16}\text{O}_{13}\text{Co}_4$ : C, 44.75; H, 1.92. Found: C, 44.92; H, 2.13.

*meso*-9: 2.9 mg was obtained (5.4%). *d,l*-9: 21 mg was obtained (39.0%). The ratio of *d,l*-9:*meso*-9 was equal to 88:12 (by weight), de 76%. Spectral and physicochemical characteristics are identical with those reported earlier.<sup>4f</sup>

**Reduction with Cobaltocene.** Under an atmosphere of nitrogen,  $\text{HBF}_4\cdot\text{Me}_2\text{O}$  (201 mg, 1.5 mmol) was added dropwise to a solution of alcohol **1** (52 mg, 0.125 mmol) and alcohol **2** (56 mg, 0.125 mmol) in dry ether (20 mL) at  $-20^\circ\text{C}$ . The reaction mixture was stirred for 1 h, and the ethereal layer was removed. At  $-20^\circ\text{C}$ , cations **3** and **4** were washed with dry ether ( $2 \times 15$  mL), the residual solvent was removed under reduced pressure, and the precipitate was dissolved in dry  $\text{CH}_2\text{Cl}_2$  (5 mL). Cobaltocene (47 mg, 0.25 mmol) was added at  $0^\circ\text{C}$ , the reaction mixture was stirred at  $20^\circ\text{C}$  for 3 h, then an additional amount of cobaltocene (9 mg, 0.05 mmol) was introduced, and stirring was continued for an additional hour (TLC control). By NMR of the crude mixture, the product contribution was equal to **7:8:9**, 33:38:29. The ratio of *d,l*- and *meso*-diastereoisomers of **7**, **8**, and **9** was equal to 78:22 (de 56%), 70:30 (de 40%), and 75:25 (de 50%), respectively.

**One-Step, THF-Mediated Dimerization.** Under an atmosphere of nitrogen, at  $-5^\circ\text{C}$ ,  $\text{HBF}_4\cdot\text{Me}_2\text{O}$  (62 mg, 0.5 mmol) was added dropwise to a solution of alcohol **1** (52 mg, 0.125 mmol), alcohol **2** (56 mg, 0.125 mmol), and THF (36 mg, 40.5  $\mu\text{L}$ , 0.5 mmol) in dry  $\text{CH}_2\text{Cl}_2$  (5 mL). The reaction mixture was stirred at  $20^\circ\text{C}$  for 8 h (TLC control). The reaction mixture was cooled to  $0^\circ\text{C}$ , diluted with ether (15 mL), and washed with water ( $4 \times 10$  mL). The ethereal layer was dried ( $\text{MgSO}_4$ ), filtered through a short bed of silica gel (2 cm), and evaporated to dryness under reduced pressure. By NMR of the crude mixture, the product distribution was equal to **7:8:9**, 26:49:25. The ratio of *d,l*- and *meso*-diastereoisomers of **7**, **8**, and **9** was equal to 92:8 (de 84%), 94:6 (de 88%), and 95:5 (de 90%), respectively.

**One-Step,  $\text{Tf}_2\text{O}$ -Mediated Dimerization.** Under an atmosphere of nitrogen, at  $-5^\circ\text{C}$ ,  $\text{Tf}_2\text{O}$  (141 mg, 84  $\mu\text{L}$ , 0.5 mmol) was added dropwise to a solution of alcohol **1** (52 mg, 0.125 mmol) and alcohol **2** (56 mg, 0.125 mmol) in dry  $\text{CH}_2\text{Cl}_2$  (5 mL). The reaction mixture was stirred at  $20^\circ\text{C}$  for 24 h (TLC control). The reaction mixture was cooled to  $0^\circ\text{C}$  and diluted with ether (10 mL) and water (5 mL). The organic layer was repeatedly washed with water ( $5 \times 4$



mL). The ethereal layer was dried ( $\text{Na}_2\text{SO}_4$ ), then filtered through a short bed of silica gel (2 cm) and evaporated to dryness under reduced pressure. By NMR of the crude mixture, the product distribution was equal to **7**:**8**:**9**, 19:47:34. The ratio of *d,l*- and *meso*-diastereoisomers of **7**, **8**, and **9** was equal to 88:12 (de 76%), 94:6 (de 88%), and 96:4 (de 92%), respectively.

**[1-Phenyl-3-(4'-methoxyphenyl)-2-propyn-1-ol]dicobalthexacarbonyl (12)**. Under an atmosphere of nitrogen, a solution of BuLi in hexane (4.8 mmol, 3 mL/1.6 M) was added dropwise to a solution of 1-ethynyl-4-methoxybenzene (0.598 g, 4.4 mmol) in dry THF (10 mL) at  $-20^\circ\text{C}$  (10 min). Upon addition, the reaction mixture was stirred at  $-20^\circ\text{C}$  for 5 h, and a solution of benzaldehyde (0.53 mL, 5.2 mmol) was added dropwise to the reaction mixture at  $-40^\circ\text{C}$  (15 min). The reaction mixture was stirred 19 h at ambient temperature, then cooled to  $0^\circ\text{C}$  and quenched with  $\text{H}_2\text{O}$  (30 mL) and saturated  $\text{NH}_4\text{Cl}$  (30 mL). An aqueous layer was extracted with ether ( $3 \times 15$  mL), and combined ethereal fractions were dried over  $\text{Na}_2\text{SO}_4$ . Upon concentration under reduced pressure (1/3 of the initial volume), under an atmosphere of nitrogen, the crude alcohol (1.04 g, 4.4 mmol; assuming 100% yield) was added to a solution of dicobaltoctacarbonyl (1.65 g, 4.8 mmol) in THF (80 mL). The reaction mixture was stirred at room temperature for 15 h, concentrated under reduced pressure, and fractionated on a silica gel column (153 g, PE:E, 5:1) to afford **12** (1.99 g, 86.5%) as black crystals (crystallizes in a freezer in 2 weeks). Mp:  $80\text{--}88^\circ\text{C}$  (sealed capillary; coevaporated with benzene,  $3 \times 1$  mL). TLC (benzene/acetone, 9:1):  $R_f$  0.60.  $^1\text{H}$  NMR (200 MHz,  $\text{CDCl}_3$ ):  $\delta$  2.49 (1H, d, OH,  $J = 2.8$ ), 3.85 (3H, s, OMe), 6.15 (1H, d, CH), 6.90 (2H, d, arom. H,  $J = 8.8$ ), 7.29–7.37 (3H, m, arom. H), 7.50 (4H, t, arom. H,  $J = 7.2$ ). MS-FAB+:  $m/z$   $\text{M}^+ 524$ ,  $507$  ( $\text{M}^+ - \text{OH}$ ),  $496$  ( $\text{M}^+ - \text{CO}$ ),  $479$  ( $\text{M}^+ - \text{OH} - \text{CO}$ ),  $468$  ( $\text{M}^+ - 2\text{CO}$ ),  $440$  ( $\text{M}^+ - 3\text{CO}$ ),  $423$  ( $\text{M}^+ - \text{OH} - 3\text{CO}$ ),  $412$  ( $\text{M}^+ - 4\text{CO}$ ),  $384$  ( $\text{M}^+ - 5\text{CO}$ ),  $356$  ( $\text{M}^+ - 6\text{CO}$ ),  $221$  ( $\text{M}^+ - \text{Co}_2(\text{CO})_6 - \text{OH}$ ). Anal. Found: C, 50.26; H 2.80.  $\text{C}_{23}\text{H}_{16}\text{O}_9\text{Co}_2$  requires: C, 50.42; H 2.69.

***d,l*- and *meso*-[1,6-Di(4'-methoxyphenyl)-3,4-diphenyl-2,5-hexadiyne]bis(dicobalthexacarbonyl) (16)**. Under an atmosphere of nitrogen,  $\text{HBF}_4\cdot\text{Me}_2\text{O}$  (458 mg, 3.42 mmol) was added dropwise to a solution of propargyl alcohol **12** (300 mg, 0.57 mmol) in dry ether (20 mL) at  $-5^\circ\text{C}$ . The reaction mixture was stirred for 2 h, an ethereal layer was removed, and the cation **13** was washed with dry ether ( $2 \times 20$  mL). The residual ether was removed under reduced pressure, and the precipitate was dissolved in  $\text{CH}_2\text{Cl}_2$  (11.4 mL). The reaction mixture was then treated with zinc (222 mg, 3.42 mmol) and stirred at ambient temperature for 16 h (TLC control). Zinc was filtered off, and the crude mixture was fractionated on the silica gel column (27 g; PE:E, 9:1) to afford **16** (157 mg, 54.2%; *d,l:meso*, 93:7, de 86%), as black crystals (crystallizes in a freezer in 2 weeks). TLC (PE:E, 9:1): *d,l*  $R_f$  0.36; *meso*  $R_f$  0.42;  $T_{\text{dec}}$   $125\text{--}130^\circ\text{C}$  (partial melting; sealed capillary; coevaporated with benzene,  $3 \times 1$  mL).  $^1\text{H}$  NMR (400 MHz,  $\text{CDCl}_3$ ):  $\delta$  3.83 (6H, s, 2OMe), *meso*-**16** 4.82 (2H, s, 2CH), *d,l*-**16** 5.18 (2H, s, 2CH), *meso*-**16** 6.63 (4H, d, arom. H,  $J = 8.8$ ), *d,l*-**16** 6.84 (4H, d, arom. H,  $J = 8.8$ ), 6.96–7.05 (8H, m, arom. H), 7.10 (4H, t, arom. H,  $J = 7.6$ ), 7.25 (2H, t, arom. H,  $J = 7.2$ ). MS-FAB+:  $m/z$   $\text{M}^+ 930$  ( $\text{M}^+ - 3\text{CO}$ ),  $846$  ( $\text{M}^+ - 6\text{CO}$ ),  $818$  ( $\text{M}^+ - 4\text{CO}$ ),  $762$  ( $\text{M}^+ - 9\text{CO}$ ),  $678$  ( $\text{M}^+ - 12\text{CO}$ ),  $647$  ( $\text{M}^+ - 12\text{CO} - \text{OCH}_3$ ),  $619$  ( $\text{M}^+ - 12\text{CO} - \text{Co}$ ),  $588$  ( $\text{M}^+ - 12\text{CO} - \text{OCH}_3 - \text{Co}$ ),  $560$  ( $\text{M}^+ - 12\text{CO} - 2\text{Co} - \text{CC}_6\text{H}_4\text{OMe}$ ),  $501$  ( $\text{M}^+ - 12\text{CO} - 3\text{Co}$ ),  $221$  ( $\text{M}^+ - 3\text{CO} - \text{HCC}_6\text{H}_5\text{CCC}_6\text{H}_4\text{OMe}$ ). Anal. Found: C, 51.84; H 2.85.  $\text{C}_{44}\text{H}_{26}\text{O}_{14}\text{Co}_4$  requires: C, 52.12; H 2.58. Single crystals suitable for X-ray structure analysis (Figure 2) were obtained by methanol vapor diffusion into a solution of *d,l*-**16** in acetone.

**X-ray Crystallography of *d,l*-16**. The crystal was mounted on a glass fiber and placed directly into the cold stream of an Oxford Diffraction Xcaliber3 diffractometer. A total of 61 450 reflections

(10 063 independent,  $R = 0.0538$ ) were collected and used for the unit cell determination and the structure refinement.<sup>9</sup> An initial Patterson map located the four cobalt atoms, while all other non-hydrogen atoms were located in the difference maps through subsequent rounds of least-squares refinement. Hydrogen atoms were placed in calculated positions with the exception of hydrogens H3 and H4, which were located in the difference map. All non-hydrogen atoms were refined anisotropically, calculated hydrogen atoms were refined as riding atoms, while H3 and H4 were refined isotropically. Structure solution and refinement were performed using Shelx97 through the Wingx interface.<sup>9</sup>

***d,l*- and *meso*-(3,4-Diphenyl-1,5-hexadiyne)bis(dicobalthexacarbonyl) (7), *d,l*- and *meso*-[1-(4'-Methoxyphenyl)-3,4-diphenyl-1,5-hexadiyne]bis(dicobalthexacarbonyl) (15), and *d,l*- and *meso*-[1,6-Di(4'-methoxyphenyl)-3,4-diphenyl-2,5-hexadiyne]bis(dicobalthexacarbonyl) (16). Reduction with Zinc**. Substrates' molar ratio 2:1 (a total of 0.25 mmol): Under an atmosphere of nitrogen,  $\text{HBF}_4\cdot\text{Me}_2\text{O}$  (201 mg, 1.50 mmol) was added dropwise to a solution of propargyl alcohols **1** (70 mg, 0.167 mmol) and **12** (44 mg, 0.083 mmol) in dry ether (20 mL) at  $-20^\circ\text{C}$ . The reaction mixture was stirred for 1.5 h, an ethereal layer was removed, and the cations **3** and **13** were washed with dry ether ( $2 \times 15$  mL). The residual ether was removed under reduced pressure, and the precipitate was dissolved in dry  $\text{CH}_2\text{Cl}_2$  (5 mL). The reaction mixture was then treated with zinc (98 mg, 1.50 mmol) and stirred at ambient temperature for 1 h (TLC control). Zinc was filtered off, and the product composition was determined by NMR to be equal to **7**:**15**:**16**, 52:24:24. The stereoisomeric ratio was determined as follows: *d,l*-**7:meso**-**7**, 78:22 (de 56%); *d,l*-**15:meso**-**15**, 70:30 (de 40%); *d,l*-**16:meso**-**16**, 70:30 (de 40%). Individual diastereoisomers were isolated by fractionation on preparative TLC plates (silica gel,  $20 \times 20$  cm; 2 plates; PE:E, 20:1): fraction 1 *d,l*-**7** and *meso*-**7**; fraction 2 *d,l*-**15**, *meso*-**15**, and  $\text{MeOC}_6\text{H}_4\text{C}\equiv\text{CCH}_2\text{C}_6\text{H}_5$  [ $\text{Co}_2(\text{CO})_6$ ] (**18**); fraction 3 *d,l*-**16** and *meso*-**16**.

Fraction 1 (*d,l*-**7** + *meso*-**7**): 42 mg was obtained (62.2%) as a red solid. TLC (PE:E, 5:1):  $R_f$  0.78. By NMR, the ratio of *d,l*-**7:meso**-**7** was equal to 80:20, de 60%. Spectral and physicochemical characteristics are identical with those reported earlier.<sup>4b</sup>

Fraction 2 (*d,l*-**15** + *meso*-**15** + **18**): by NMR data, the ratio of (*d,l*-**15** + *meso*-**15**):**18** was equal to 95:5 and the stereoisomeric ratio of *d,l*-**15:meso**-**15** was equal to 70:30, de 40%. *d,l*-**15** and *meso*-**15** were separated from trace amounts of **18** by using preparative TLC (PE/ $\text{CH}_2\text{Cl}_2$ , 15:1; 3 runs). An authentic sample of **18** was synthesized by quenching the cation **13** with tributyltin hydride.

*d,l*-**15** + *meso*-**15**: 4.7 mg was obtained (6.2%; *d,l:meso*, 70:30; de 40%) as a dark red oil. TLC (PE:E, 5:1): *d,l*-**15**  $R_f$  0.69, *meso*-**15**  $R_f$  0.69.  $^1\text{H}$  NMR (400 MHz,  $\text{CDCl}_3$ ; contains residual amount of solvents):  $\delta$  *meso*-**15** 3.83 (3H, s, OMe), *d,l*-**15** 3.86 (3H, s, OMe), *meso*-**15** 4.58 (H, d, CH,  $J = 11.2$ ), *meso*-**15** 4.69 (H, s,  $\text{C}\equiv\text{C}-\text{H}$ ), *d,l*-**15** 4.71 (H, d, CH,  $J = 5.6$ ), *meso*-**15** 4.77 (H, d, CH,  $J = 11.2$ ), *d,l*-**15** 4.86 (H, d, CH,  $J = 5.6$ ), 5.83 (H, s,  $\text{C}\equiv\text{C}-\text{H}$ ), *meso*-**15** 6.68 (2H, d, arom.,  $J = 8.8$ ), *d,l*-**15** 6.86 (2H, d, arom.,  $J = 8$ ), *meso*-**15** 6.84–7.02 (4H, m, 2H, arom.), *d,l*-**15** + *meso*-**15** 7.05–7.6 (20H, m, 10H, arom.). MS-FAB+:  $m/z$   $\text{M}^+ 824$  ( $\text{M}^+ - 3\text{CO}$ ),  $796$  ( $\text{M}^+ - 4\text{CO}$ ),  $768$  ( $\text{M}^+ - 5\text{CO}$ ),  $740$  ( $\text{M}^+ - 6\text{CO}$ ),  $712$  ( $\text{M}^+ - 7\text{CO}$ ),  $684$  ( $\text{M}^+ - 8\text{CO}$ ),  $656$  ( $\text{M}^+ - 9\text{CO}$ ),  $628$  ( $\text{M}^+ - 10\text{CO}$ ),  $600$  ( $\text{M}^+ - 11\text{CO}$ ),  $572$  ( $\text{M}^+ - 12\text{CO}$ ),  $482$  ( $\text{M}^+ - 12\text{CO} - \text{C}_7\text{H}_6$  or  $\text{C}_6\text{H}_2\text{O}$ ),  $454$  ( $\text{M}^+ - 12\text{CO} - 2\text{Co}$ ),  $395$  ( $\text{M}^+ - 12\text{CO} - 3\text{Co}$ ),  $221$  ( $\text{M}^+ - 12\text{CO} - 4\text{Co} - \text{C}_{16}\text{H}_{13}\text{O}$ ). HR-MS/FAB: calcd for  $\text{C}_{34}\text{H}_{20}\text{O}_{10}\text{Co}_4$   $\text{M}^+ - 3\text{CO}$  823.838438, found 823.841500.

$\text{MeOC}_6\text{H}_4\text{C}\equiv\text{CCH}_2\text{C}_6\text{H}_5$  [ $\text{Co}_2(\text{CO})_6$ ] (**18**): dark red solid. TLC (PE:E, 5:1):  $R_f$  0.69.  $^1\text{H}$  NMR (400 MHz,  $\text{CDCl}_3$ ):  $\delta$  3.86 (3H, s, OMe), 6.15 (1H, d, CH), 4.29 (2H, s,  $\text{CH}_2$ ), 6.92 (2H, d, arom. H,  $J = 8.8$ ), 7.29–7.37 (3H, m, arom. H), 7.50 (4H, t, arom. H,  $J =$

7.2). MS-FAB+:  $m/z$   $M^+$  508, 480 ( $M^+ - CO$ ), 452 ( $M^+ - 2CO$ ), 424 ( $M^+ - 3CO$ ), 396 ( $M^+ - 4CO$ ), 368 ( $M^+ - 5CO$ ), 340 ( $M^+ - 6CO$ ), 281 ( $M^+ - 6CO - Co$ ), 221 ( $M^+ - Co_2(CO)_6 - H$ ). HR-MS/FAB: calcd for  $C_{21}H_{14}O_6Co_2$  ( $M^+ - CO$ ) 479.945434, found 479.945900.

Fraction 3 (*d,l*-**16** + *meso*-**16**): 20 mg was obtained (46.6%). By NMR, the stereoisomeric ratio of *d,l*-**16**:*meso*-**16** was equal to 70:30, de 40%.

Substrates' molar ratio 1:1 (**1** 0.125 mmol, **12** 0.125 mmol; a total of 0.25 mmol): **7:15:16**, 39:16:45 (NMR); *d,l*-**7**:*meso*-**7**, 85:15 (de 70%); *d,l*-**15**:*meso*-**15**, 74:26 (de 48%); *d,l*-**16**:*meso*-**16**, 72:28 (de 44%). Substrates' molar ratio 3:1 (**1** 0.1875 mmol, **12** 0.0625 mmol; a total of 0.25 mmol): **7:15:16**, 63:21:17 (NMR); *d,l*-**7**:*meso*-**7**, 83:17 (de 66%); *d,l*-**15**:*meso*-**15**, 72:28 (de 44%); *d,l*-**16**:*meso*-**16**, 67:33 (de 34%). Substrates' molar ratio 7:1 (**1** 0.2188 mmol, **12** 0.0312 mmol; a total of 0.25 mmol): **7:15:16**, 83:8:9 (NMR); *d,l*-**7**:*meso*-**7**, 85:15 (de 70%); *d,l*-**15**:*meso*-**15**, 71:29 (de 42%); *d,l*-**16**:*meso*-**16**, 67:33 (de 34%). Substrates' molar ratio 9:1 (**1** 0.225 mmol, **12** 0.025 mmol; a total of 0.25 mmol): **7:15:16**, 86:8:6 (NMR); *d,l*-**7**:*meso*-**7**, 86:14 (de 72%); *d,l*-**15**:*meso*-**15**, 71:29 (de 42%); *d,l*-**16**:*meso*-**16**, 67:33 (de 34%). Substrates' molar ratio 1:3 (**1** 0.0625 mmol, **12** 0.1875 mmol; a total of 0.25 mmol): **7:15:16**, 17:23:60 (NMR); *d,l*-**7**:*meso*-**7**, 79:21 (de 58%); *d,l*-**15**:*meso*-**15**, 70:30 (de 40%); *d,l*-**16**:*meso*-**16**, 72:28 (de 44%). Hydrogen atom abstraction product **18** was formed in minute quantities (3–7%).

**Reduction with Cobaltocene.** Under an atmosphere of nitrogen,  $HBF_4 \cdot Me_2O$  (201 mg, 1.50 mmol) was added dropwise to a solution of propargyl alcohols **1** (52 mg, 0.125 mmol) and **12** (66 mg, 0.125 mmol) in dry ether (20 mL) at  $-20$  °C. The reaction mixture was stirred for 1 h, an ethereal layer was removed, and the cations **3** and **13** were washed with dry ether ( $2 \times 15$  mL). The residual amount of ether was removed under reduced pressure, and the precipitate was dissolved in  $CH_2Cl_2$  (3 mL). A solution of  $Cp_2Co$  (70.9 mg, 0.375 mmol) was prepared by dissolving  $Cp_2Co$  in  $CH_2Cl_2$  (2 mL) and stirring it at room temperature under anaerobic conditions (20 min). This solution was then added dropwise to the reaction flask at 0 °C. The reaction was stirred for 3 h (TLC controlled). The crude mixture was then filtered through a short bed of Florisil (2 cm) and eluted with ether. Ether was stripped by reduced pressure, and the crude solid was analyzed using a spectroscopic method. By NMR, the product distribution was equal to **7:15:16**, 47:47:6. The stereoisomeric ratio was determined as follows: *d,l*-**7**:*meso*-**7**, 76:24 (de 52%); *d,l*-**15**:*meso*-**15**, 70:30 (de 40%); *d,l*-**16**:*meso*-**16**, 57:43 (de 14%).

*d,l*-**7** and *meso*-**7**: 11.5 mg was obtained (23%). By NMR, the ratio of *d,l*-**7**:*meso*-**7** is equal to 71:29 (de 42%).

*d,l*-**15**, *meso*-**15** and **18**: 46.2 mg was obtained (includes minute quantities of an unidentified side product). By NMR data, the ratio of *d,l*-**15** + *meso*-**15**:**18** was equal to 48:52; *d,l*-**15**:*meso*-**15**, 70:30 (de 40%). Cross-dimer **15** could not be isolated in a homogeneous form because of the presence of an unidentified component that exhibited similar chromatographic behavior.

*d,l*- and *meso*-**16**: 4.3 mg was obtained (6.78%). By NMR, the ratio of *d,l*-**16**:*meso*-**16** is equal to 66:34, de 32%.

**One-Step, THF-Mediated Dimerization.** Under an atmosphere of nitrogen, THF (36 mg, 0.50 mmol) was added to a solution of propargyl alcohols **1** (52 mg, 0.125 mmol) and **12** (66 mg, 0.125 mmol) in dry  $CH_2Cl_2$  (5 mL). The reaction mixture was then cooled to  $-5$  °C, and  $HBF_4 \cdot Me_2O$  (67 mg, 0.50 mmol) was added dropwise. The mixture was then warmed to 20 °C and stirred for 21 h (TLC control). The reaction was then cooled to 0 °C, and

ether (15 mL) was added. The organic layer was washed with  $H_2O$  ( $5 \times 10$  mL) and dried ( $Na_2SO_4$ ). The crude mixture was evaporated to dryness, then diluted with ether (20 mL) and added dropwise to a solution of  $Co_2(CO)_8$  (17 mg, 0.05 mmol) in ether (30 mL) at room temperature. The reaction was stirred for 2 h at room temperature. The crude was separated from excess  $Co_2(CO)_8$  by column chromatography using silica gel as a stationary phase (20 g; PE, E). By NMR of the crude mixture, the product distribution was equal to **7:15:16**, 53:14:33. The stereoisomeric ratio was determined as follows: *d,l*-**7**:*meso*-**7**, 92:8 (de 84%); *d,l*-**15**:*meso*-**15**, 86:14 (de 72%); *d,l*-**16**:*meso*-**16**, 82:18 (de 64%).

*d,l*-**7** and *meso*-**7**: 20 mg was obtained (40.3%). By NMR, the ratio of *d,l*-**7**:*meso*-**7** is equal to 94:6 (de 88%).

*d,l*-**15**, *meso*-**15** and **18**: 7.9 mg was obtained. By NMR data, the ratio of *d,l*-**15** + *meso*-**15**:**18** was equal to 80:20. Individual compounds were isolated by using preparative TLC (PE/ $CH_2Cl_2$ , 15:1; 3 runs). Obtained were *d,l*-**15** + *meso*-**15** (3 mg, 2.6%) and **18** (1.5 mg, 2.4%). The stereoisomeric ratio of *d,l*-**15**:*meso*-**15** is equal to 91:9 (de 82%).

**Decomplexation of *d,l*- and *meso*-16 to *d,l*- and *meso*-1,6-Di-(4'-methoxyphenyl)-3,4-diphenyl-2,5-hexadiyne (**19**).** *d,l*-**16** and *meso*-**16** were decomplexed in order to separate the individual compounds from a side product of identical chromatographic mobility. Under an atmosphere of nitrogen,  $Ce(NH_4)_2(NO_3)_6$  (89 mg, 0.162 mmol) in acetone (5 mL) was added dropwise to a solution of impure *d,l*-**16** and *meso*-**16** (21 mg, 0.0202 mmol) in acetone (5 mL) at  $-78$  °C. The reaction mixture was stirred for 1 h (TLC control), then poured, at 0 °C, onto a saturated aqueous solution of NaCl (25 mL) and extracted with ether ( $3 \times 15$  mL). The combined ethereal layers were dried ( $Na_2SO_4$ ,  $+4$  °C), the solvent, upon filtration, was stripped away under reduced pressure, and the residue was fractionated by PTLC (PE/B, 1:1). Obtained was *d,l*-**19** + *meso*-**19** (4.9 mg, 55.0%) as a yellowish-white solid. By NMR, the ratio of *d,l*-**19**:*meso*-**19** was equal to 61:39 (de 22%). The diastereomeric mixture can be crystallized, to release a white solid, by dissolving it in a mixture of  $CH_2Cl_2$  (5 mL) and pentane (15 mL), followed by coevaporation of solvents under reduced pressure. Mp: 129–130 °C (sealed capillary; coevaporated with benzene,  $3 \times 1$  mL). TLC (PE/E, 1:1):  $R_f$  0.50.  $^1H$  NMR (400 MHz,  $CDCl_3$ ):  $\delta$  *meso*-**19** 3.82 (6H, s, 2OMe), *d,l*-**19** 3.83 (6H, s, 2OMe), *meso*-**19** 4.28 (2H, s, 2CH), *d,l*-**19** 4.31 (2H, s, 2CH), 6.85 (4H, d, arom. H,  $J = 8.8$ ), 7.27–7.44 (14H, m, arom. H). MS DEI:  $m/z$  442 ( $M^+$ ), 221. HR-MS/DEI: calcd for  $C_{32}H_{26}O_2$  442.193280, found 442.193564.

**Acknowledgment.** This material is based upon work supported by the National Science Foundation under CHE-0707865. We are also greatly indebted to the Office of Graduate Studies, Research and International Programs and University Corporation, California State University Northridge, for generous support.

**Supporting Information Available:** Calculated heats of formation (kcal/mol) for propargyl cations **10**, **11**, and **17** (PM3) (Table 1; Figure 1); calculated total electronic energies (hartrees) for cobalt-complexed propargyl cations **3**, **4**, and **13** (HF/3-21G\*) (Table 1). Tables of crystallographic details, bond distances and angles, atomic coordinates, and equivalent isotropic displacement parameters, as well as torsion angles for *d,l*-**16**, are available in CIF format. This material is available free of charge via the Internet at <http://pubs.acs.org>.

OM070180M